*P h y s i c s*

# VISUALIZATION OF MICROWAVE ABSORPTION OF THE GRAPHITE PERIODICAL STRUCTURE WITH THERMOELASTIC OPTICAL MICROSCOPE

## L. ODABASHYAN

*Chair of Applied Electrodynamics and Modeling, YSU, Armenia*

This paper shows a non-destructive visualization of the absorption of microwave filed by a graphite periodic structure. The visualization system was a thermo-elastic optical indicator microscope. The article presents the interaction of the electromagnetic field with graphite cylindrical cells of periodicity and shows the distribution of the electromagnetic field over the graphite cells. Depending on the distance between the periodic structure of graphite and the microwave source, the electromagnetic field distribution and absorption rate were different. The visualization was performed using a microwave signal with a frequency of 11 *GHz* and a maximum power of 35 *dBm*.

**Introduction.** There is a lot of sophisticated research on the development of broadband microwave absorbers for military and civilian purposes that have good absorption properties over a wide frequency range with a physically thinner coating. Particularly in military applications, where radar absorbing materials (RAM) are commonly used in stealth technology to hide an object from radar detection. RAM is coated on the object so that the electrical and magnetic properties can be modified to increase the absorption of microwave energy [1–4].

Following the recent studies of materials with high microwave absorption rates, graphite was chosen as a coating layer for an object to hide from radars due to its superior conductive properties and relaxation losses. There is a lot of research studies related to the utilization of graphite as a microwave absorber, and due to that great interest,in this article the interaction between the periodic structure of graphite and the electromagnetic (EM) field was visualized using a thermoelastic optical indicator microscope (TEOIM). Periodic structures are effective for absorbing microwave fields, therefore, in this article, the material under study was chosen as a cylindrical periodic

---

* E-mail: levon.odabashyan@ysumail.am

graphite cellular structure embedded in organic glass [5–7]. This visualization method makes it possible to more vividly demonstrate the interaction of graphite with an EM field, which allows to understand and evaluate the absorption phenomena of graphite.

In this paper, we investigate the phenomenon of absorption of microwave fields in the graphite periodic structure and show the images of that distribution for different distances of EM source from graphite periodic structure. The measurements have shown that the EM fields are concentrated on each cell of graphite due to the microwave absorption properties of graphite. In the setup it was used ITO (indium tin oxide), which is an indicator of magnetic fields, therefore, only magnetic (H) fields (microwave absorption of graphite) are visualized in the article. The simulations were performed by Comsol Multiphysics and simulation results were consistent with the experimental results. This unique method of visualization may be an important and informative tool in the field of RAM research.

**Materials and Methods.** The schematic image of the experimental setup is shown in Fig. 1a. The optical indicator (OI) was the glass substrate coated by a 100 *nm* ITO thin film for heat absorption. A microwave signal was generated by a synthesized sweeper R and Sc SMA100B at the frequency of 11 *GHz* at zero power, and then amplified up to 35 *dBm* by a power amplifier Mini Circuits ZVE-3W-183+. The generated microwave signal was transmitted by a rectangular waveguide Pasternak WR-90 and interacted with the ITO thin absorbing layer placed in front of the waveguide. The frequency 11 *GHz* was chosen as the optimal frequency according to the waveguide effectivity, and this frequency is also in the X-band, which is in the range of interests of the RAM [8]. To reduce the noise level and increase the light reflection, a ceramic plate with 1 *mm* thickness was placed between the waveguide and optical indicator. With this adjustment, we get a uniform and monochrome view in the visible area of the camera. This method utilized optical components such as a light-emitting source, circular and linear polarizers, $\lambda/4$ wave-plate, and CCD camera. TEOIM setup is based on the polarized light microscope system. Tthe articles [9, 10] precisely describe the working principle of TEOIM setup numerically and theoretically, as well as the principle of software application.

Fig. 1b shows the material under test (MUT), which included an organic glass plate with a thickness of 0.3 *cm* and graphite powder. The graphite powder was condensed and placed inside the cylindrical gaps. The diameter, thickness, and distance from each other of each graphite cell were 0.5 *cm*, 0.3 *cm*, and 1 *cm*, respectively. The influence of organic glass on the EM fields could be neglected due to its dielectric properties. When the experiment was carried out with MUT, the EM filed interacted directly with periodic graphite cells and indirectly with ITO glass. The graphite cells absorbed the EM fields and transfered microwave energy into heat energy which was concentrated in each cell of graphite [11]. The heated cells acted on the ITO glass and due to the thermoelasticity effect, we were able to register this in the CCD camera and derive the final figurative pictures.

In general, microwave absorption can be described by the following equation

$$P = \frac{1}{2}\sigma[E]^2 + \pi f \varepsilon_0 \dot{\varepsilon}_r [E^2] + \pi f \mu_0 \dot{\mu}_r [H^2], \tag{1}$$
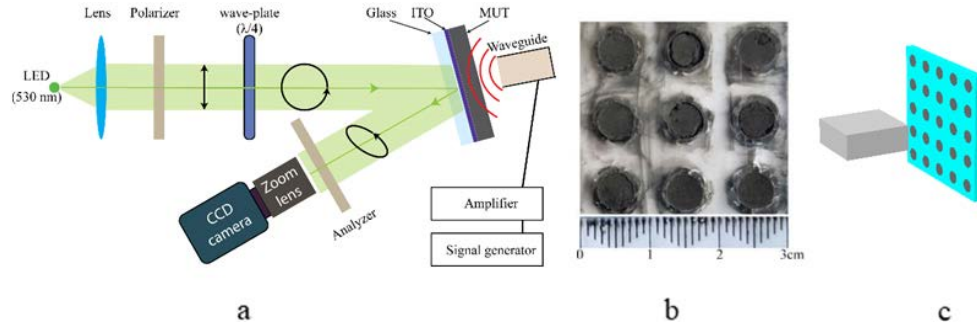
Fig. 1. a) Schematic illustration of visualization system; b) the graphite cylydrical periodic structure (MUT); c) the simulation model in COMSOL.

where $E$ is the electric field amplitude; $H$ – the magnetic field amplitude; $\sigma$ – the electrical conductivity; $f$ – microwave frequency; $(\dot{\varepsilon}_r)$ – the imaginary part of the relative permittivity; $(\dot{\mu}_r)$ – the imaginary part of relative permeability. The first, second, and third terms on the right side of Eq. (1) describe the Joule, dielectric, and magnetic losses, respectively [11].

In Fig. 1c it is shown a simulation model by Comsol Multiphysics. In the simulation process, the cylindrical dotes of graphite were chosen $5 \times 5$ (in the experiment 3/3) for a more clear demonstration. In the simulation, the dielectric property of the graphite powder was chosen from the article [12], where the dielectric properties of graphite were set in the range from 1 to 10 $GHz$.

**Results and Discussion.** Fig. 3 shows the microwave magnetic field distribution at 11 $GHz$ without (a, c) and with (b, d) MUT, where the distance between microwave source and optical indicator was 6 $mm$ (a, b) and 17 $mm$ (c, d).

As seen from Fig. 2a and 2b, the main form of the magnetic field distribution changed with a change in the distance between the radiation source to the optical indicator from 6 $mm$ to 17 $mm$. We can also see that the intensity of magnetic field distribution became weaker with increasing the distance between the microwave source and optical indicator. When placing MUT, the microwave magnetic field distribution was mainly changed, as shown in Fig. 2b and 2d. Microwave fields interact with graphite cells and are absorbed by them. It is seen from the experimental data that microwave fields were concentrated in each graphite cell. As seen from Fig. 2b and 2d, the central graphite cell has a hight intensity, which is explained by the correspondence between the waveguide center and graphite cell. When the microwave source was placed at a far distance (17 $mm$, Fig. 2d), the microwave field intensity became weaker, and this tendency showed that with increasing distance to the emitted source, the distribution of the magnetic field at the MUT would become uniform, which is an important fact for RAM technology. When the absorption becomes homogenous, the graphite periodic structure can substitute for the graphite layer in preparation for RAMs.
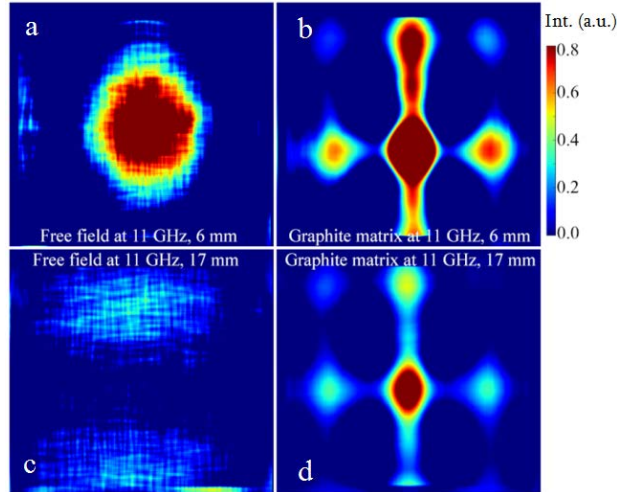
Fig. 2. The microwave magnetic field distribution at 11 *GHz* without (a, c) and with (b, d) MUT, where the distance between microwave source and optical indicator was 6 *mm* (a, b) and 17 *mm* (c, d).
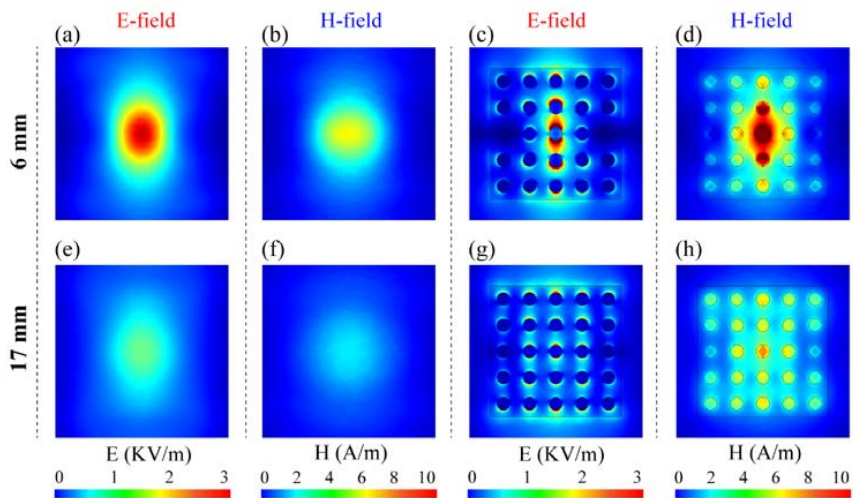


Fig. 3. The simulation result of microwave electromagnetic field distribution at 6 *mm* distance for free field (a, b) and with MUT (c, d), and at 17 *mm* distance for free field (e, f) and with MUT (g, h).

Fig. 3 shows the results of simulation of the electromagnetic field distribution of the microwave range when the microwave source and the optical indicator were located at a distance of 6 *mm* (a, b, c, d) and 17 *mm* (e, f, g, h), respectively.

Fig. 3 (a, b, e, f) shows the simulation results of electromagnetic field distribution without MUT (free field), and this clearly shows the abatement of the intensity of

the free electromagnetic field with a change in the distance between the microwave source and the optical indicator from 6 *mm* to 17 *mm*. Fig. 3 (c, d, g, h) shows the simulation electromagnetic field distribution with MUT, from where we can see the decrease in intensity when the distance of the microwave source and optical indicator changes from 6 *mm* to 17 *mm*. As shown in the real experiment, the simulation results also show that by placing the microwave field in the far distance the electromagnetic field distribution becomes more homogenous. Note that in simulation the graphite powders cells array was made by $5 \times 5$ to derive more descriptive results.

Simulations were performed by Comsol Multiphysics to observe the average distribution of the EM field of the MUT as a function of graphite cell thickness, period (distance between cell centers), and radius. The simulation revealed cell thicknesses of 0.3 *cm*, 0.5 *cm*, and 0.7 *cm*.

The simulation results for the average intensity of the electric field were 536 *V/m*, 625 *V/m* and 690 *V/m*, and of the magnetic field were 1.83 *A/m*, 1.56 *A/m*, and 1.33 *A/m*, for the thicknesses of 0.3 *cm*, 0.5 *cm*, and 0.7 *cm* , respectively. During the simulation, the period of the cells changed from 0.3 *cm* to 0.7 *cm* with a step of 0.2 *cm*, the average electric field intensity was 568 *V/m*, 536 *V/m*, and 508 *V/m* respectively, and a magnetic field intensity was 1.70 *A/m*, 1.83 *A/m*, 1.96 *A/m*, respectively. Finally, the cell radii of 0.15 *cm*, 0.25 *cm*, and 0.35 *cm* were observed, the average intensity of the electric field was 618 *V/m*, 536 *V/m*, and 419 *V/m*, and magnetic field intensity was 1.93 *A/m*, 1.83 *A/m*, and 1.57 *A/m*, respectively. The simulation results showed that with an increase in the thickness of the graphite cells, the average intensity of the electric field increased, while the magnetic field intensity decreased. When the period of the graphite cells was increased, the average electric field intensity showed a decreasing behavior, while the average magnetic field intensity increased. As the cell radius increased, the mean electric and magnetic fields intensities began to exhibit decreasing behavior.

**Conclusion.** The microwave absorption in the graphite periodic structure was visualized by the non-contact and non-destructive TEOIM visualization technique. According to the experimental results, we found out that the microwave absorption intensity varies greatly depending on the distance between the graphite periodic structure and radiation source. The total image of the microwave field distribution of the graphite powders cells became more homogenous when microwave sources were placed at a far distance. TEOIM exhibits great potential, including high resolution, high sensitivity, and fast inspection for visualization of microwave absorption of periodic structural material such as graphite. This technique can be an important tool in the field of RAM research.

# R E F E R E N C E S

1. Xie S., Zhu L., et al. Three-dimensional Periodic Structured Absorber for Broadband Electromagnetic Radiation Absorption. *Electron. Mater. Lett.* **16** (2020), 340–346.
https://doi.org/10.1007/s13391-020-00219-y

2. Jiang W., Yan L., et al. Electromagnetic Wave Absorption and Compressive Behavior of a Three-dimensional Metamaterial Absorber Based on 3D Printed Honeycomb. *Sci. Rep.* **8** (2018), Article No: 4817.
https://doi.org/10.1038/s41598-018-23286-6

3. Delfini A., Albano M., et al. Advanced Radar Absorbing Ceramic-Based Materials for Multifunctional Applications in Space Environment. *Materials* **11** (2018), Article No: 1730.
https://doi.org/10.3390/ma11091730

4. Gill N., Puthucheri S., et al. Critical Analysis of Frequency Selective Surfaces Embedded Composite Microwave Absorber for Frequency Range 2–8 GHz. *J. Mater. Sci.: Mater. Electron.* **28** (2017), 1259–1270.
https://doi.org/10.1007/s10854-016-5654-3

5. Rusly, S.N.A., Matori, K.A., et al. Microwave Absorption Properties of Single- and Double-layer Coatings Based on Strontium Hexaferrite and Graphite Nanocomposite. *J. Mater. Sci.: Mater. Electron.* **29** (2018), 14031–14045.
https://doi.org/10.1007/s10854-018-9535-9

6. Chen X., Jia X., et al. A Graphite-based Metamaterial Microwave Absorber. *IEEE Antennas Wirel. Propag. Lett.* **18** (2019), 1016–1020.
https://doi.org/10.1109/LAWP.2019.2907780

7. Guo Z., Huang H., et al. Microwave Properties of the Singlelayer Periodic Structure Composites Composed of Ethylene-vinyl Acetate and Polycrystalline Iron Fibers. *Sci. Rep.* **7** (2017), Article No: 11331.
https://doi.org/10.1038/s41598-017-11884-9

8. Kumar A., Singh S. Development of Coatings for Radar Absorbing Materials at X-band. *IOP Conf. Ser.: Mater. Sci. Eng.* **330** (2018), Article No: 012006.
https://doi.org/10.1088/1757-899X/330/1/012006

9. Baghdasaryan Zh., Babajanyan A., et al. Visualization of Microwave Heatingformesh-Patterned Indium-tin-Oxide by a Thermo-Elastic Optical Indicator Microscope. *Arm. J. Phys.* **11** (2018), 175–179.

10. Baghdasaryan Zh., Babajanyan A., et al. Thermal Distribution in Unidirectional Carbon Composite Material Due to the Direct Heating and Microwave Influence Visualized by a Thermo-elastic Optical Indicator Microscope. *Measurement* **151** (2020), Article No: 107189.
https://doi.org/10.1016/j.measurement.2019.107189

11. Chandrasekaran S., Basak T., Srinivasan R. Microwave Heating Characteristics of Graphite-based Powder Mixtures. *Int. Commun. Heat Mass Transf.* **48** (2013), 22–27.
https://doi.org/10.1016/j.icheatmasstransfer.2013.09.008

12. Hotta M., Hayashi M., et al. Complex Permittivity of Graphite, Carbon Black and Coal Powders in the Ranges of X-band Frequencies (8.2 to 12.4 GHz) and between 1 and 10 GHz. *ISIJ International* **51** (2011), 1766–1772.
https://doi.org/10.2355/isijinternational.51.1766

Լ. ՕԴԱԲԱՇՅԱՆ

ՄԻԿՐՈԱԼԻՔԱՅԻՆ ՏԻՐՈՒՅԹՈՒՄ ԳՐԱՖԻՏԻ ՊԱՐԲԵՐԱԿԱՆ ՀԱՄԱԿԱՐԳԻ
ԿԼԱՆՄԱՆ ԱՐՏԱՊԱՏԿԵՐՈՒՄԸ ՋԵՐՄԱԱՌԱՁԳԱԿԱՆ ՕՊՏԻԿԱԿԱՆ
ՄԱՆՐԱԴԻՏԱԿԻ ՄԻՋՈՑՈՎ

Աշխատանքում ներկայացված է միկրոալիքային տիրույթում գրաֆիտի
պարբերական համակարգի կլանման անհիում արտապատկերումը ջերմաէլաս-
տիկ օպտիկական մանրադիտակի օգնությամբ: Ներկայացված է էլեկտրամագնի-
սական դաշտի փոխագդեցությունը գրաֆիտի զլանաձև պարբերական բջիջների
հետ և ցույց է տրված էլեկտրամագնիսական դաշտի բաշխումը գրաֆիտի բջիջնե-
րի վրա: Կախված գրաֆիտի պարբերական կառուցվածքի՝ միկրոալիքային աղ-
բյուրից ունեցած հեռավորությունից, էլեկտրամագնիսական դաշտի բաշխվա-
ծությունները և կլանման ինտենսիվությունները տարբեր են: Արտապատկերումը
իրականացվել է 11 GHz հաճախությամբ և 35 dBm հգորությամբ միկրոալիքային
ազդանշանի դեպքում:

Л. ОДАБАШЯН

ВИЗУАЛИЗАЦИЯ МИКРОВОЛНОВОГО ПОГЛОЩЕНИЯ ГРАФИТОВОЙ
ПЕРИОДИЧЕСКОЙ СИСТЕМЫ С ПОМОЩЬЮ ТЕРМОУПРУГОГО
ОПТИЧЕСКОГО МИКРОСКОПА

В работе представлена неразрушающая визуализация поглощения
микроволнового поля периодической структурой графита с помошью тер-
моупругий оптический микроскопа. В статье представлено взаимодействие
электромагнитного поля с графитовыми цилиндрическими ячейками и
показано распределение электромагнитного поля по графитовым ячейкам.
В зависимости от удаленности периодической структуры графита от мик-
роволнового источника распределение и интенсивность поглощения элек-
тромагнитного поля были разными. Визуализация производилась с по-
мощью микроволнового сигнала с частотой 11 GHz и максимальной мощ-
ностью 35 dBm.